Journal of Sound and Vibration (2002) **256**(2), 287–297
doi:10.1006/jsvi.2001.4209, available online at http://www.idealibrary.com on IDEAL®

CRACK IDENTIFICATION IN BEAM STRUCTURES USING MECHANICAL IMPEDANCE

Y. Bamnios

T.E.I. of Thessaloniki, Faculty of Technological Applications, Department of Electronics, P.O. Box 14561, *GR*-541 01 *Thessaloniki, Greece*

AND

E. Douka and A. Trochidis

Physics Division, School of Technology, Aristotle University of Thessaloniki, GR-54006 *Thessaloniki, Greece. E-mail: troxidis@eng.auth.gr*

(*Received* 21 *June* 2001, *and in final form* 19 *November* 2001)

The influence of a transverse open crack on the mechanical impedance of cracked beams under various boundary conditions is investigated both analytically and experimentally. It is shown that the driving-point impedance changes substantially due to the presence of the crack and the changes depend on the location and the size of the crack and on the force location. Monitoring the change of the first antiresonance as a function of the measuring location along the beam, a jump in the slope of the plot in the vicinity of the crack occurs. The magnitude of the jump depends on the crack size. Experimental results are presented from tests on Plexiglas beams damaged at different locations and different magnitudes and are found to be in good agreement with theoretical predictions. Based on the results of the present work, an efficient prediction scheme for accurate crack localization is proposed.

1. INTRODUCTION

Cracks present a serious threat to the performance of structures. Most of the failures of presently used equipment are due to material fatigue. For this reason, methods allowing early detection and localization of cracks have been the subject of intensive investigations. As a result, a variety of analytical, numerical and experimental investigations now exist.

A crack in a structure induces a local flexibility and this affects the dynamic behavior of the whole structure to a considerable degree. It results in reduction of natural frequencies and changes in mode shapes of vibration. An analysis of these changes makes it possible to identify cracks. In the pioneering work of Dimarogonas [1] and Paipetis and Dimarogonas [2] the crack is modelled as a local flexibility and the equivalent stiffness was computed using fracture mechanics methods. This calculation enabled further the construction of a compliance matrix for the crack [3]. It was concluded that the bending term in the crack compliance matrix was dominant if the beam dimensions satisfied the Bernoulli–Euler theory. In that vein, Chondros and Dimarogonas [4] developed methods to identify cracks in various structures relating the crack depth to the change in natural frequencies for known crack position. Adam and Cawley [5] developed an experimental technique to estimate the location and depth of a crack from changes in natural frequencies. Gudmunson [6] used a perturbation method to predict changes in natural frequencies of structures resulting from

0022-460X/02/$35.00

cracks, notches and other geometrical changes. Further research on crack identification via natural frequency changes, was carried out by Anifantis *et al.* [7]. They found that one could find the size and position of large cracks if the changes in the first two natural frequencies were known. Ostachowicz and Krawczuk [8] examined the effect of more than one crack on the natural frequencies of a cantilever beam. Using a similar model Masoud *et al.* [9] investigated the vibrational characteristics of a prestressed fixed–fixed beam with a symmetric crack and the coupling effect between crack depth and axial load. Rizos *et al.* [10] suggested a method for using measured amplitudes at two points of a cantilever beam vibrating in one of its natural modes to identify crack location and depth. Narkis [11] simulated the crack by an equivalent spring connecting the two segments of a cracked beam and developed a closed-form solution, which he applied to the study of the inverse problem of localization of cracks on the basis of natural frequency measurements. A different approach to the problem of cracked beams, has been used by Chondros *et al.* [12]. They developed a continuous vibration theory of cracked Bernoulli–Euler beams and reported experimental results for the variation of the fundamental frequency of a simply supported cracked beam. Armon *et al.* [13] proposed a method for detection and localization of slots and cracks based on rank-ordering of the modes according to the reduction of natural frequencies. They have shown that rank-ordering of the eigenfrequency shifts is a function of the damage location but does not depend on the damage magnitude for small cracks.

Some researches have been looking at the steady state response of a beam to a simple harmonic input including the non-linear effects of crack closure. Actis and Dimarogonas [14] noted some non-linear features of the spectra. Chu and Shen [15] made an analogy between a cracked beam and a bilinear spring–mass system. Their method centered around forcing a cracked beam at low frequency and observing the superharmonic components. The presence of superharmonic components in the Fourier spectrum has been proposed as an indicator of the discontinuity in stiffness resulting from a crack.

Sundermeyer and Weaver [16] used the weakly non-linear character of a cracked vibrating beam for crack localization. The proposed approach is based on examining the response of a bilinear mass–spring system to excitation at two frequencies such that the difference between the two frequencies is the resonant frequency.

In searching for an additional defect information carrier for crack appearance, the use of the mechanical impedance was introduced by Bamnios and Trochidis [17] in the case of a cracked cantilever beam. It was shown that the mechanical impedance changes substantially due to the presence of a crack and these changes follow definite trends with the crack parameters and force location. An attempt has been made to relate the changes of the impedance form and magnitude to crack location with limited success. It turned out that using these parameters no reliable criterion for crack localization could be adopted. Prabhakar *et al.* [18] further investigated the changes in mechanical impedance in the case of cracked rotor-bearing systems and they suggested that it could be used for crack detection.

In the present work, the influence of a transverse surface crack on the driving-point impedance of beams under different boundary conditions is investigated both analytically and experimentally. The crack is modelled by the appropriate equivalent spring connecting the two segments of the beam. Analysis of this approximate models, results in algebraic equations, which relate the changes in mechanical impedance to the location and characteristics of the crack. It is shown that the mechanical impedance changes substantially due to the presence of the crack in case of flexural vibrations. The changes follow definite trends depending upon the location of the crack and consequently can provide the information required for accurate crack localization.

2. MATHEMATICAL MODELLING

2.1. CANTILEVER BEAM

The physical system under consideration, shown in Figure 1, is a beam of uniform rectangular cross-section with a crack located at a position x_c. The crack is assumed to be open and have a uniform depth. For general loading, a local flexibility matrix relates displacements and forces. In the present analysis, since only bending vibrations are considered, the rotational crack compliance is assumed to be dominant in the local flexibility matrix [3].

The bending spring constant K_T in the vicinity of the cracked section when a transverse crack of uniform depth a exists, is given by [2]

$$K_T = \frac{1}{c}, \; c = (5{\cdot}346\, w/EI)\, J(a/w), \tag{1}$$

where w is the depth of the beam, E is the modulus of elasticity of the beam, I is the area moment of inertia for the beam cross-section and $J(a/w)$ the dimensionless local compliance function.

Different functional forms for the compliance function have been proposed, according to the symmetry of the crack [2, 8]. In a recent publication [19] two forms of this function were used and was concluded that the best results were achieved using the one proposed by Paipetis and Dimarogonas [2]. Therefore, in this paper, this function is used. It has the form

$$J(a/w) = 1{\cdot}8624(a/w)^2 - 3{\cdot}95(a/w)^3 + 16{\cdot}37(a/w)^4 - 37{\cdot}226(a/w)^5 + 76{\cdot}81(a/w)^6$$
$$- 126{\cdot}9(a/w)^7 + 172(a/w)^8 - 43{\cdot}97(a/w)^9 + 66{\cdot}56(a/w)^{10}. \tag{2}$$

Due to localized crack effect, the cracked beam can be simulated as two uniform beams joined together by a torsional spring at the crack location [11] (Figure 2).

A driving force $F = F_0 e^{j\omega t}$ is considered acting on the beam. Thus, the location of the driving force and the location of the crack divide the beam in three parts. Depending on the location of the driving force, one has to solve two problems with different boundary conditions to calculate the displacements $n(x)$ of the beam.

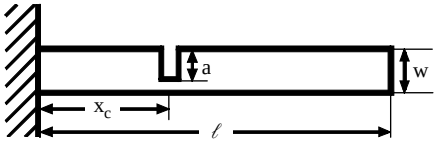

Figure 1. Cantilever beam under study.

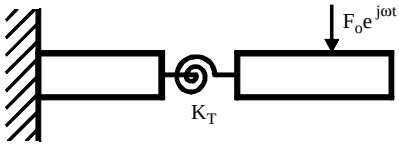

Figure 2. Cracked cantilever beam model.

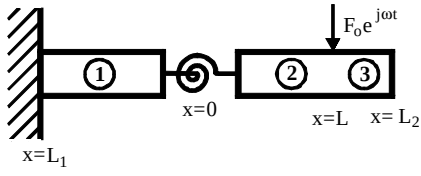

Figure 3. Cracked cantilever beam with driving force between free end and crack.

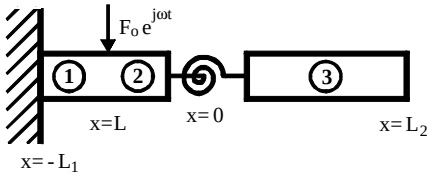

Figure 4. Cracked cantilever beam with driving force between crack and clamped end.

For a driving force between free end and crack the geometry is shown in Figure 3. The displacement on each part of the beam is

$$\begin{aligned}
&\text{Part 1: } n_1(x) = c_1 \cosh K_B x + c_2 \sinh K_B x + c_3 \cos K_B x + c_4 \sin K_B x,\\
&\text{Part 2: } n_2(x) = c_5 \cosh K_B x + c_6 \sinh K_B x + c_7 \cos K_B x + c_8 \sin K_B x,\\
&\text{Part 3: } n_3(x) = c_9 \cosh K_B x + c_{10} \sinh K_B x + c_{11} \cos K_B x + c_{12} \sin K_B x
\end{aligned} \tag{3}$$

with $K_B^4 = \omega^2 \rho A l^4 / EI$, where l is the total length of the beam, A is the cross-sectional area, ω is the vibration angular velocity, ρ is the material density and c_i, $i = 1, 2, \ldots, 12$ are the constants to be determined from the boundary conditions.

The boundary conditions for this case in both ends are:

$$\begin{aligned}
&\text{at } x = -L_1\text{: } n_1(-L_1) = 0, \qquad n_1'(-L_1) = 0,\\
&\text{at } x = L_2\text{: } M_3(L_2) = 0, \qquad F_3(L_2) = 0,
\end{aligned} \tag{4}$$

where prime denotes derivative with respect to x.

The continuity conditions at the crack position and the compatibility condition due to rotational flexibility are:

$$\begin{aligned}
&\text{at } x = 0\text{: } n_1(0) = n_2(0),\ M_1(0) = M_2(0),\ F_1(0) = F_2(0)\\
&-EI \frac{\partial^2}{\partial x^2} n_1(0) = K_T \left[\frac{\partial}{\partial x} n_1(0) - \frac{\partial}{\partial x} n_2(0) \right]
\end{aligned} \tag{5}$$

and the conditions at the force location are:

$$\text{at } x = L\text{: } n_2(L) = n_3(L),\ n_2'(L) = n_3'(L),\ M_2(L) = M_3(L),\ F_2(L) - F_3(L) = F_0. \tag{6}$$

For a driving force between crack and clamped end the geometry is shown in Figure 4. This case can be treated similarly by considering the appropriate boundary conditions. Finally, in case of a crack at the clamped end, the beam is divided in two parts (see Figure 5) with different boundary conditions.

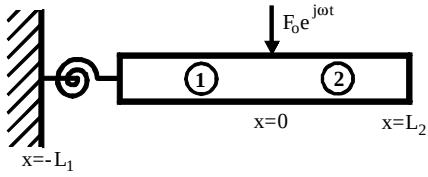

Figure 5. Cantilever beam cracked at the clamped end.

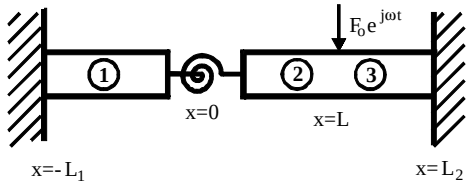

Figure 6. Cracked beam clamped at both ends.

The resulting characteristic equations, for the above mentioned three cases can be solved numerically and both the eigenfrequencies and the mechanical impedance of the beam at different positions can be obtained. The excitation force is shifted along the beam and the displacement is calculated at the application point. Consequently, the driving-point impedance of the beam at an arbitrary location x can be derived according to the relation $Z(x) = F_0/j\,2\pi f n(x)$, where $n(x)$ is the corresponding displacement and f is the frequency.

2.2. BEAM CLAMPED AT BOTH ENDS

The geometry of this case is shown in Figure 6 and the corresponding boundary conditions are:

$$\text{at } x = -L_1\text{: } n_1(-L_1) = 0,\ n_1'(-L_1) = 0,$$

$$\text{at } x = L_2\text{: } n_2(L_2) = 0,\ n_2'(L_2) = 0,$$

$$\text{at } x = L\text{: } n_1(L) = n_2(L),\ n_1'(L) = n_2'(L),$$

$$M_1(L) = M_2(L),\ F_1(L) - F_2(L) = F_0,$$

$$\text{at } x = 0\text{: } n_2(0) = n_3(0),\ M_2(0) = M_3(0),\ F_2(0) = F_3(0),$$

$$-EI\frac{\partial^2}{\partial x^2}n_2(0) = K_T\left[\frac{\partial}{\partial x}n_2(0) - \frac{\partial}{\partial x}n_3(0)\right]. \tag{7}$$

The resulting characteristic equation can be solved numerically to obtain the driving-point impedance at an arbitrary location along the beam as described in the previous section.

3. NUMERICAL RESULTS

Using the analytical results obtained in the previous section, the driving-point mobility of cracked beams under different boundary conditions was calculated. Instead of the

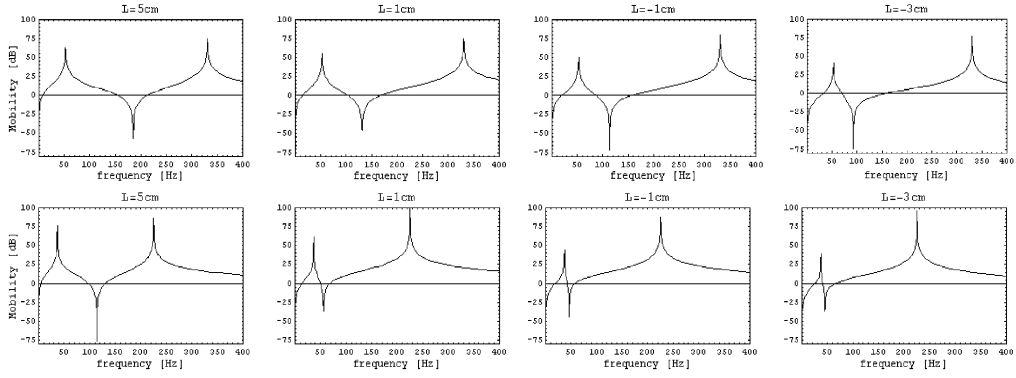

Figure 7. Predicted mechanical mobility of a cantilever beam at different positions along a 35 cm long plexiglas beam of rectangular cross-section $2 \times 2\,cm^2$ (a) uncracked, (b) cracked (crack depth: 80%, crack location: 20 cm from free end).

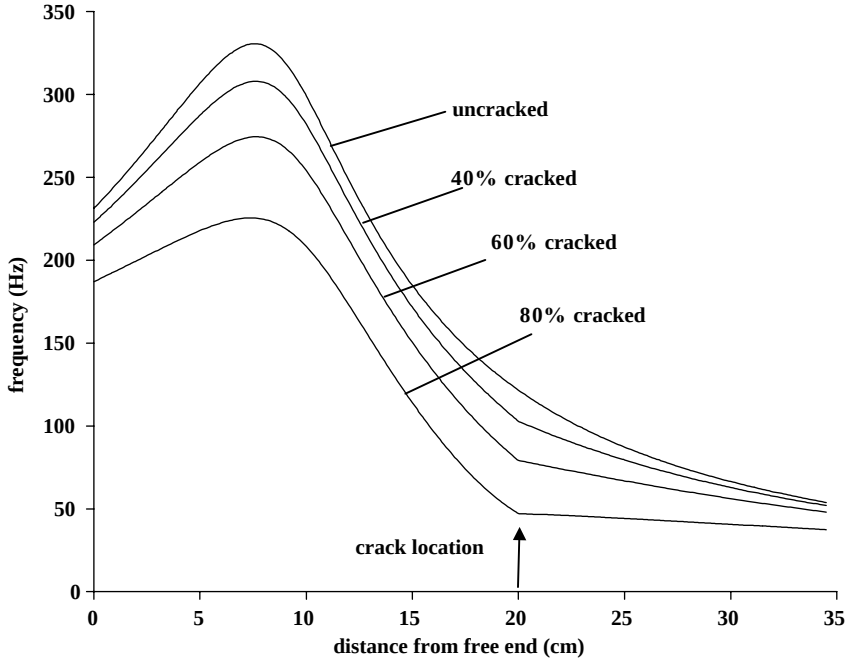

Figure 8. Predicted changes in the first antiresonance of a 35 cm long cracked cantilever beam versus measuring location (crack depth: 40, 60 and 80%, crack location: 20 cm from free end).

impedance, the mobility was calculated for convenience, since mobility can be easier to measure. In order to investigate the influence of the measuring point on the mobility, the location of the crack and its depth were kept constant and the driving force was systematically shifted along the beam.

Figure 7 shows the predicted mechanical mobility at different positions along a 35 cm cantilever Plexiglas beam of rectangular cross-section $2 \times 2\,cm^2$ for a crack depth of 80%.

An extreme crack depth was selected for convenience in order to magnify the changes. The crack was located 20 cm from the free end. The expected reduction in natural frequencies of vibration compared to the uncracked beam is evident. The main result,

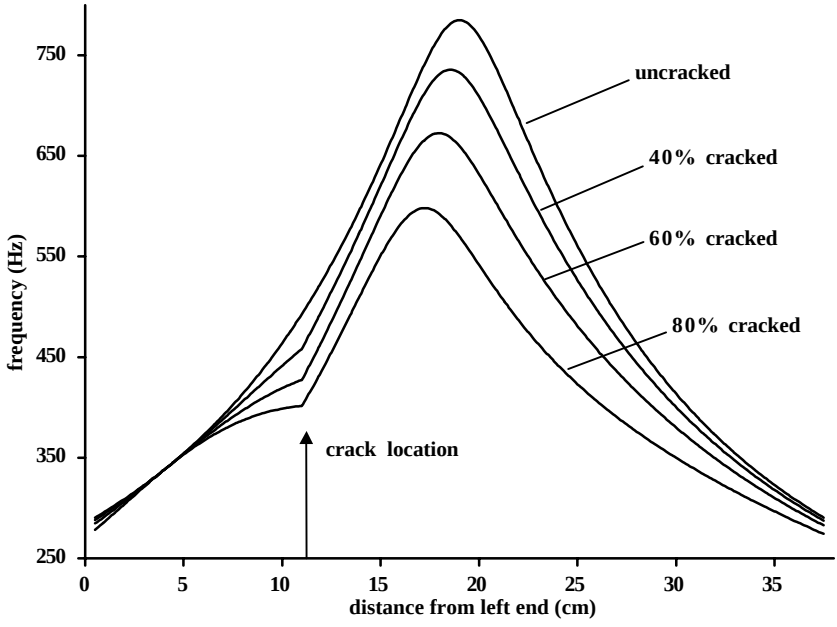

Figure 9. Predicted changes in the first antiresonance of a 38 cm long cracked beam clamped at both ends versus measuring location for different crack depths (crack location: 11 cm from left clamped end).

however, is that the first antiresonance moves towards the first resonance as the driving point approaches the crack. In the vicinity of the crack tends to coincide with the first resonance. After crossing the crack, the position of the antiresonance remains unchanged. On the contrary, in case of an uncracked beam, the first antiresonance moves smoothly towards the first resonance.

Figure 8 shows the predicted change in the first antiresonance of the same cantilever beam as a function of the measuring location along the beam for different crack depths. It can be seen that the influence of a crack on the mechanical impedance of the beam strongly depends on the crack's location. In the vicinity of the crack there is a jump in the slope of the curve depending on crack's depth. The abrupt change in the slope of the curve is due to the fact that in the case of a cracked beam the first antiresonance remains unchanged after crossing the crack.

Figure 9 shows the predicted change in the antiresonance of the same beam clamped at both ends as a function of the measuring location for different crack depths. In the vicinity of the crack there is a jump in the slope of the curve depending on crack's depth quite similar to the one in case of a cantilever beam.

4. EXPERIMENTAL INVESTIGATION

In order to validate the approximate model used in the analysis, a series of measurements were undertaken on plexiglas beams. The beams used in the experiments had square cross-section $2 \times 2\,\text{cm}^2$ and were cut from bars of commercial plexiglas. The crack was modelled by sawing cuts. It is known from the literature that the frequencies measured on a sawed beam might be different from those on cracked beams. The difference depends crucially on the width of the cut [20].

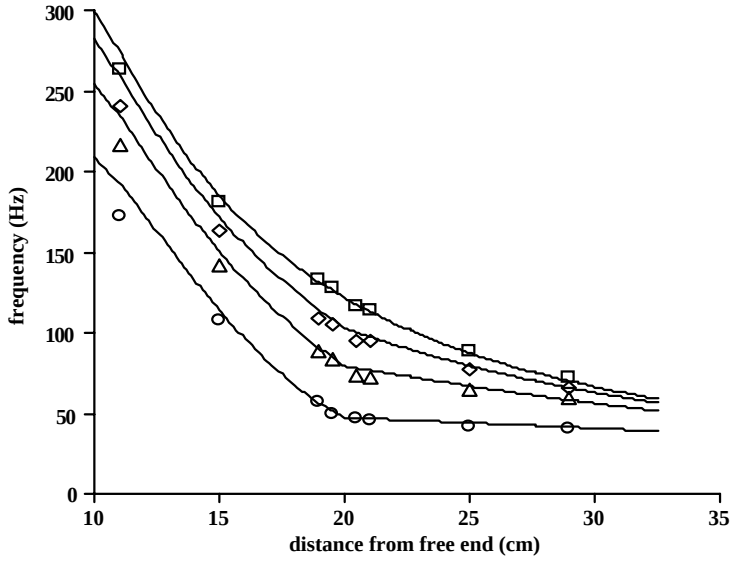

Figure 10. Change of the first antiresonance of a 35 cm long cracked cantilever beam versus measuring location along the beam for different crack depths. Comparison between prediction and measurements (crack location: 20 cm from free end). □, Uncracked; ◇, crack 40%; △, crack 60%; ○, crack 80%.

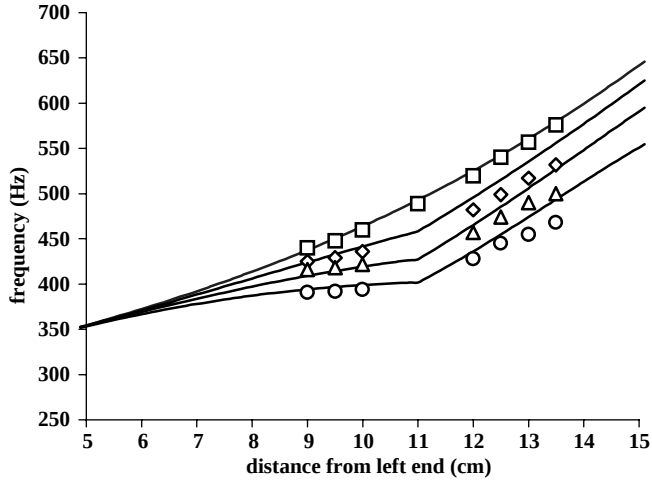

Figure 11. Change of the first antiresonance of a 38 cm long clamped–clamped beam versus measuring point along the beam for different crack depths. Comparison between prediction and measurements (crack location: 11 cm from left end). □, Uncracked; ◇, crack 40%; △, crack 60%; ○, crack 80%.

Therefore, we have tried to achieve as narrow saw cuts as possible. The saw cuts in the experiments, made on a lathe, were of the order of 0·3–0·4 mm and since a 20% crack corresponds to a depth of 4 mm the ratio a/w is, in the worst case, of the order of 0·1. As it follows from reference [20], in this case the difference Δf of the frequencies between slots and cracks are negligible. Clamping of the beams was secured through the use of two heavy steel jaws. The beams were forced into oscillations by a 15 mm diameter voice coil weighing 5 g.

attached to the beam. The coil was placed in the field of a permanent magnet and was excited by a waveform oscillator (B&K 2010). The driving force was kept constant and was shifted and the velocity measured at different locations along the beam. The signals were transferred to an analyzer to give plots of the driving-point mobility versus frequency. The whole experimental set-up allowed the reproducibility of the results.

Several beams with the same geometry and material, cracked at different positions were tested under different boundary conditions. The mechanical mobility was measured in steps of 10 mm. Using the mobility plots, the position of the first antiresonance at each location was estimated.

A typical plot of the antiresonance value as a function of the measuring position is shown in Figure 10. This figure shows that in case of a cracked cantilever beam the change in the first antiresonance is not smooth. It exhibits a jump in the slope of the curve in the vicinity of the crack. The magnitude of the jump depends on the crack depth. Figure 11 shows the corresponding results for the same beam clamped at both ends. In this case again the change in the first antiresonance is not smooth. There is an abrupt jump in the slope of the curve in the vicinity of the crack depending on the crack depth. The agreement between the results of predictions and measurements in all cases was very good. Moreover, the consistency of the experimental results in all cases tested was adequate.

5. CONCLUSIONS

The effect of a transverse surface crack on the mechanical impedance of cracked beams under different boundary conditions was investigated both analytically and experimentally. It was shown that, far from the expected changes in natural frequencies, the mechanical impedance changes substantially. The changes depend on the location and the size of the crack. Thus, the driving-point mechanical impedance can be used as an additional defect information carrier, which complementary with natural frequencies changes can be used for crack identification.

Based on impedance measurements an efficient prediction scheme for crack location can be proposed. Starting from one end and moving towards the other the impedance will be measured and the shift of the first antiresonance will be estimated. In the vicinity of the crack the antiresonance coincides with the first resonance. After crossing the crack location, the antiresonance remains fairly constant. Thus, the crack exists in the neighborhood of the location where there is a jump in the slope of the curve of the antiresonance shift versus measuring position. The method can be used to locate the crack roughly and then other methods can be employed to determine the crack characteristics more precisely. The method lacks accuracy for small cracks $a/w < 0{\cdot}20$. This confines the range of application of the method to moderate cracks only. In most practical cases, however, a 20% crack is not usually an indication of immediate failure. The results of this work can be easily extended to include more complex structures and boundary conditions. Further work is already under way to explore the application of the proposed method to more complicated structures. These include multicracked beams and cracked plates.

REFERENCES

1. A. DIMAROGONAS 1976 *Vibration Engineering*. St. Paul, Minesota: West Publishers.
2. S. A. PAIPETIS and A. D. DIMAROGONAS 1986 *Analytical Methods in Rotor Dynamics*. London: Elsevier Applied Science.

3. G. GOUNARIS and A. D. DIMAROGONAS 1988 *Computers and Structures* **28**, 309–313. A finite element of a cracked prismatic beam for structural analysis.
4. T. G. CHONDROS and A. D. DIMAROGONAS 1980 *Journal of Sound and Vibration* **69**, 531–538. Identification of cracks in welded joints of complex structures.
5. A. D. ADAMS and P. CAWLEY 1979 *Journal of Strain Analysis* **14**, 49–57. The location of defects in structures from measurements of natural frequencies.
6. P. GUDMUNDSON 1982 *Journal of Mechanics and Physics of Solids* **30**, 339–353. Eigenfrequency changes of structures due to cracks, notches or other geometrical changes.
7. N. ANIFANTIS, P. RIZOS and A. DIMAROGONAS 1985 *American Society of Mechanical Engineers, Design Division Publication* DE **7**, 189–197. Identification of cracks by vibration analysis.
8. W. M. OSTACHOWICZ and M. KRAWCZUK 1991 *Journal of Sound and Vibration* **150**, 191–201. Analysis of the effect of cracks on the natural frequencies of a cantilever beam.
9. S. MASOUD, M. A. JARRAD and M. AL-MAAMORY 1998 *Journal of Sound and Vibration* **214**, 201–212. Effect of crack depth on the natural frequency of a prestressed fixed–fixed beam.
10. P. RIZOS, N. ASPRAGATHOS and A. D. DIMAROGONAS 1990 *Journal of Sound and Vibration* **138**, 381–388. Identification of crack location and magnitude in a cantilever beam from the vibration modes.
11. Y. NARKIS 1994 *Journal of Sound and Vibration* **172**, 549–558. Identification of crack location in vibrating simple supported beam.
12. T. G. CHONDROS, A. D. DIMAROGONAS and J. YAO 1998 *Journal of Sound and Vibration* **218**, 17–34. A continuous cracked beam vibration theory.
13. D. ARMON, Y. BEN-HAIM and S. BRAUN 1994 *Mechanical Systems and Signal Processing* **8**, 81–91. Crack detection in beams by rank-ordering of eigenfrequency shifts.
14. R. I. ACTIS and A. D. DIMAROGONAS 1989 12th *ASME Conference on the Mechanical Engineering, Vibration and Noise, Montreal, Canada.* Non-linear effects due to closing cracks in vibrating beams.
15. Y. CHU and M. SHEN 1992 *American Institute of Aeronautics and Astronautics Journal* **30**, 2512–2519. Analysis of forced bilinear oscillators and the application to cracked beams.
16. J. N. SUNDERMEYER and R. L. WEAVER 1995 *Journal of Sound and Vibration* **183**, 857–871. On crack identification and characterization in a beam by non-linear vibration analysis.
17. G. BAMNIOS and A. TROCHIDIS 1995 *Journal of Acoustical Society of America* **97**, 3625–3635. Mechanical impedance of a cracked cantilever beam.
18. S. PRABHAKAR, A. S. SEKHAR and A. R. MOHANTYY 2001 *Journal of Acoustical Society of America* **110**, 2351–2359. Detection and monitoring of cracks using mechanical impedance of rotor-bearing systems.
19. F. G. TOMASEL, H. A. LARRONDO and P. A. A. LAURA 1999 *Journal of Sound and Vibration* **228**, 1195–1204. Detection of cracks in cantilever beams: experimental set-up using optical techniques and theoretical modelling.
20. P. CAWELY and R. RAY 1988 *Journal of Vibration, Acoustics, Stress and Reliability in Design, Transactions of the American Society of Mechanical Engineers* **110**, 366–370. A comparison of the natural frequency changes produced by cracks and slots.

APPENDIX A: NOMENCLATURE

A	cross-sectional area
a	crack depth
c	compliance
c_i	constants
E	modulus of elasticity of the beam material
F	driving force
F_0	amplitude of the driving force
f	frequency
I	moment of inertia of beam cross-section
J	dimensionless local compliance function
K_B	wavenumber for bending waves
K_T	bending spring constant
l	length of the beam
L_1	distance of clamped end from the crack

L_2	distance of free end from the crack
L	distance of the driving force from the crack
M	bending moment
n	displacement
w	depth of the beam
ρ	material density
ω	vibration angular velocity